Investigation of a Bacterial Pore-forming Chimera Toxin for Application as a Novel Drug-delivery System Tool

ATSUSHI TABATA[1*], YUKIMASA OHKUBO[1*], ERIKO SAKAKURA[1*], TOSHIFUMI TOMOYASU[1], KAZUTO OHKURA[2] and HIDEAKI NAGAMUNE[1]

[1]*Department of Biological Science and Technology, Life System, Institute of Technology and Science, The University of Tokushima Graduate School, Tokushima, Japan;*
[2]*Faculty of Pharmaceutical Sciences, Suzuka University of Medical Science, Suzuka, Mie, Japan*

Abstract. *Background/Aim: Cholesterol-dependent cytolysins (CDCs) are pore-forming toxins from Gram-positive bacteria. The aim of this study was to investigate the potential of a CDC, intermedilysin, as a drug-delivery system (DDS) for clinical application. Materials and Methods: Intermedilysin was modified by the addition of a disulfide bridge to regulate pore formation, by swapping domain 4 to provide cholesterol-binding capacity, and by the introduction of a targeting domain. The resultant chimera protein, His-LTBP-CDC(ss)^{IP}, was investigated for its use as a DDS tool in vitro. Results: His-LTBP-CDC(ss)^{IP} exhibited a regulated pore-forming capacity under reducing conditions. This chimera protein was able to deliver a drug-carrier liposome specifically to the target cell, to be endocytosed into the cell with subsequent release of the components into the cytoplasm. Conclusion: A chimera protein derived from the bacterial pore-forming toxin intermedilysin (His-LTBP-CDC(ss)^{IP}) forms the basis for a novel DDS tool.*

Drug-delivery systems (DDS) are new therapeutic technologies improving the controlled distribution and action of drugs. A DDS approach requires three fundamental technologies: the specific delivery of the drug(s) to the target cells, the controlled release of the drug from the drug carrier and an improved drug absorption into the target cells. When applied to cancer treatment a DDS is expected to promote efficient therapy and to improve the quality of life of the patients. A wide range of strategies for DDSs have been reported (1-5), with some applications based on the utilization of bacterial toxins (6).

Cholesterol-dependent cytolysins (CDCs) are a family of bacterial pore-forming exotoxins secreted from various pathogenic Gram-positive bacteria. A typical CDC is composed of four domains: domains 1-3 (1D-3D) contribute to the formation of the membrane pore and domain 4 (4D) to toxin binding to the target cell membrane (7). The overall mode of action of a CDC involves; i) the initial association of 4D with its receptor (membrane cholesterol for a typical CDC); ii) the association of membrane-bound monomeric CDC units to form an oligomeric ring structure, called a pre-pore; iii) a conformational change in the CDC, especially in domain 3 (3D); and finally iv) the insertion of the structurally changed 3D into the target cell membrane, resulting in a pore (approximate diameter of 25 to 30 nm) composed of 35 to 50 monomers of CDC.

Investigations have been carried out in our laboratory on streptococcal CDCs including intermedilysin (ILY), *Streptococcus mitis*-derived human platelet aggregation factor (Sm-hPAF) and streptolysin O (SLO), secreted by the oral commensal *Streptococcus intermedius* (8), *Streptococcus mitis* Nm-65 isolated from a patient with Kawasaki disease (9), and *Streptococcus pyogenes*, respectively. In the context of CDC protein engineering, it has been reported that in perfringolysin O and SLO, the introduction of a disulfide bridge between domains 2D and 3D can prevent the structural change required for pore formation (10, 11). This inhibitory effect on pore-formation can be reversed by cleavage of the disulfide bridge under reducing conditions to recover full pore-formation activity, similar to that of the non-modified wild-type CDC. This control over CDC pore formation by the introduction of a disulfide bridge between 2D and 3D can be potentially exploited for controlled drug release from a drug carrier. Interestingly, the newly reported

*These Authors contributed equally to this work.

Correspondence to: Hideaki Nagamune, Department of Biological Science and Technology, Life System, Institute of Technology and Science, The University of Tokushima Graduate School, 2-1, Minamijosanjima-cho, Tokushima, Tokushima 770-8506, Japan. Tel/Fax: +81 886567525, e-mail: nagamune@bio.tokushima-u.ac.jp

Key Words: Cholesterol-dependent cytolysin, drug-delivery system, chimera toxin.

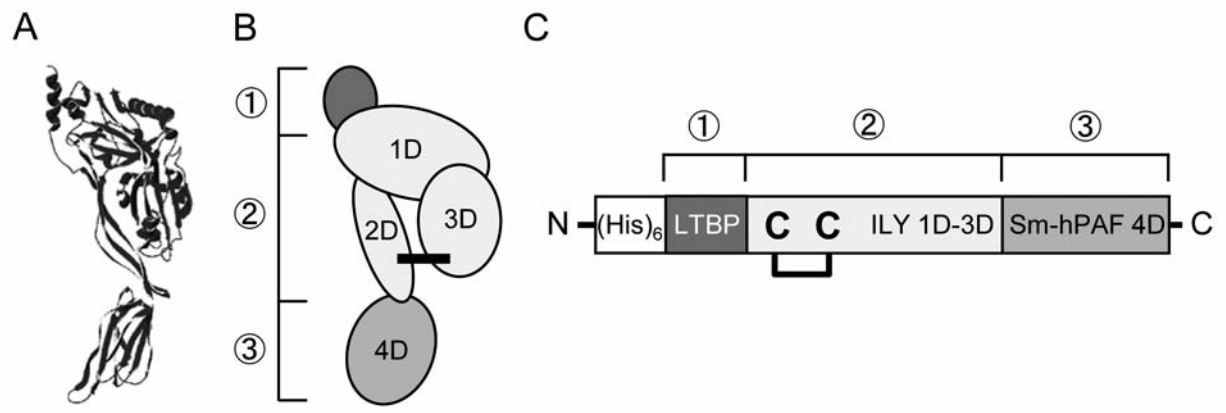

Figure 1. *Molecular design of a recombinant chimera protein (His-LTBP-CDC(ss)^{IP}) as a drug-delivery system (DDS) tool with controlled pore-formation ability using cholesterol-dependent cytolysins (CDC). A: Three-dimensional model of intermedilysin (ILY). B: Schematic representation of His-LTBP-CDC(ss)^{IP}. The protein is composed of targeting domain ①, functional domains responsible for controlled pore-forming activity ②, and binding domain to carriage (drug carrier such as liposome) containing anticancer drugs ③. C: Schematic representation of the primary structure of His-LTBP-CDC(ss)^{IP}. The numbers correspond to the description given in B. This recombinant chimera protein has N-terminal hexa His-tag to facilitate purification, lung tumor-binding peptide (LTBP) to function as the targeting domain, 1D to 3D of ILY with two substitutions to Cys as the functional domains, and 4D of Sm-hPAF for the domain for binding to cholesterol-containing membranes.*

CDC, Sm-hPAF/lectinolysin (LLY) (12, 13), has been shown to be structurally unique, with a fifth domain as the *N*-terminal domain, in addition to the 'core' structure of typical CDCs composed of four domains. This structural information suggests that it should be possible to introduce an additional domain into the *N*-terminal region of a CDC without affecting its function. Therefore, we hypothesized that attachment of a ligand molecule, such as an antibody or a peptide, with affinity to target cells to a CDC with in-built conformational restriction, due to the introduction of a disulfide bridge between 2D and 3D [CDC(ss)], would result in the production of an effective drug-delivery 'vehicle'.

In this study, we designed and constructed a novel chimera protein for DDS application using the CDC ILY as the base molecule (Figure 1). Several modifications were carried out in order to construct a chimera protein, including introduction of a disulfide bridge between 2D and 3D, swapping of 4D from ILY to Sm-hPAF, and appending of the lung tumor-binding peptide (LTBP) (14) onto the *N*-terminal of the CDC(s). The purified chimera protein was evaluated for its utility as a DDS.

Materials and Methods

Construction of expression vectors for recombinant chimera proteins. The expression vector for the recombinant chimera protein as a model DDS tool (designated as His-LTBP-CDC(ss)^{IP}, Figure 1) was constructed using pQE-1 (QIAGEN, Hilden, Germany) with a modified multi-cloning site, *Bam*HI-*Apa*I-*Sal*I-*Sac*I-*Eco*RI-*Pst*I-*Sma*I-*Sfi*I-*Not*I-*Sph*I. The DNA fragments encoding LTBP (14) and the chimera CDC were prepared as described below then inserted into the vector at the *Bam*HI-*Sph*I site. Briefly, the insert encoding LTBP was prepared by a cassette ligation method using six oligonucleotides (GATCCGATGACGGTCTGC, TGCGTTGCAGA CCGTCATCG, AACGCATCACAGCGTCAAGCACACGCACAG, C G T A G C C T G T G C G T G T G C T T G A C G C T G T G A , GCTACGGCTGTATCGCTTGC, GGCCGCAAGCGATACAGC) and the resultant fragment had the *Bam*HI site in the 5'-end and the *Not*I site at the 3'-end. The other insert encoding chimera CDC was prepared as follows. Amplification and introduction of two point mutations, G83C and S217C, of the fragment encoding a region from 1D to 3D of ILY was carried out by polymerase chain reaction (PCR) with the cloned *ily* gene from *S. intermedius* UNS46 (GenBank ID: AB029317) as a template. The fragment encoding 4D of Sm-hPAF was also amplified with the cloned *sm-hpaf* gene from *S. mitis* Nm-65 (GenBank ID: AB051299) as a template. These fragments were joined by fusion PCR and the resultant fragment encoding the chimera CDC had the *Not*I site at the 5'-end and the SphI site at the 3'-end. The fragments with proper restriction sites (*Bam*HI-*Not*I for LTBP fragment and *Not*I-*Sph*I for the chimera CDC fragment) were inserted into the *Bam*HI-*Sph*I double-digested vector. In addition, the expression vector for a reference molecule His-CDC(ss)^{IP}, lacking the LTBP part in His-LTBP-CDC(ss)^{IP}, was also constructed. After confirmation of the DNA sequence of the constructed vectors, *Escherichia coli* DH5α Z1 was transformed by each vector and the expression of recombinant chimera proteins was confirmed by sodium dodecylsulphate-polyacrylamide gel electrophoresis (SDS-PAGE) and Coomassie Brilliant Blue R-250 (CBB) staining of transformants after isopropyl-β-D(–)-thiogalactopyranoside (IPTG)-induction.

Expression and purification of recombinant chimera proteins. The expression of His-tagged recombinant chimera proteins, designated as His-LTBP-CDC(ss)^{IP} and His-CDC(ss)^{IP} in log-phase bacteria, were induced by incubation with IPTG (final concentration 0.1-1.0 mM) in Luria-Bertani (LB) broth containing 50 μg/ml ampicillin, for 3 to 4 h. Purification of the proteins was conducted by standard

nickel-affinity chromatography of the bacterial cell lysate. Briefly, bacterial cells were washed with phosphate-buffered saline (PBS), re-suspended in sonication buffer [PBS, containing 20% sucrose, 1 mM EDTA and 2 mg/ml lysozyme, or 20 mM sodium phosphate buffer (pH 7.4) containing 20 mM imidazole and 500 mM NaCl] and sonicated under cooling in an ice bath. The cell lysate was centrifuged (8,600 ×*g*, 10 min, 4˚C) and the supernatant was applied to nickel-affinity chromatography column using Ni-NTA agarose (QIAGEN) or HisTrap HP (GE Healthcare, Buckinghamshire, England). The purity of the recovered His-tagged recombinant proteins was checked by CBB staining after SDS-PAGE, and the concentration of the purified proteins was determined using Bradford reagent (Bio-Rad, Hercules, CA, USA).

Evaluation for membrane-binding capacity of recombinant chimera proteins. The preparation of erythrocyte membrane was conducted as follows: human erythrocytes (from healthy volunteers) washed with PBS, were lysed by suspension in 5 mM Tris-HCl (pH 7.5), then washed five times with the same hypotonic buffer, and re-suspended in PBS. The purified His-tagged recombinant chimera proteins were incubated with or without erythrocyte membranes at 37˚C for 1 h, then centrifuged (13,200 ×*g*, 10 min, 4˚C). The resultant supernatant and pellet were electrophoresed by SDS-PAGE, blotted onto polyvinylidene difluoride (PVDF) membrane and the chimera proteins were detected by a monoclonal antibody against 1D-3D of ILY previously prepared in our laboratory.

Controlled pore-formation under reduced conditions. The hemolytic activity of His-LTBP-CDC(ss)^{IP}, was assayed in PBS containing 0.5% (v/v) of human erythrocytes and 10 mM dithiothreitol (DTT). After incubation at 37˚C for 1 h and centrifugation, the OD_{540} of the supernatant was measured in a microplate reader (Model 550; Bio-Rad), and the hemolytic activity was calculated as previously described (8). For evaluation of the hemolytic properties under physiological reducing conditions, the hemolytic activity was also measured under the presence of reduced-glutathione (GSH).

Cell-targeting ability of His-LTBP-CDC(ss)^{IP}. In order to prepare a DDS model, Nile-Red-labeled human erythrocytes were incubated with His-LTBP-CDC(ss)^{IP} at 37˚C for 1 h in PBS containing 1% bovine serum albumin (BSA). The Nile-Red labeled human erythrocytes were prepared as follows: Human erythrocytes washed with PBS were incubated with PBS containing 50 μM Nile-Red at room temperature for 30 min. The labeled erythrocytes were washed three times with PBS then twice with PBS containing 1% BSA, and re-suspended in PBS containing 1% BSA for the binding experiment.

Both human lung carcinoma cell line A549 (RCB0098; Riken Bioresource Center, Tsukuba, Japan) and a human normal fibroblast cell line NB1RGB (RCB0222; Riken Bioresource Center) were cultured in Dulbecco's modified eagle's medium (DMEM) containing 10% fetal bovine serum and antibiotics (penicillin G and streptomycin) at 37˚C under 5% CO_2. These cells were inoculated into 6-well cell culture plates at 2×10^5 cells/well for A549 and 1×10^5 cells/well for NB1RGB respectively, and were cultured for 48 h. The erythrocytes bound to His-LTBP-CDC(ss)^{IP} were added to the cells and were incubated for 1 h, then washed three times with PBS. The cells were observed using a fluorescence microscope (Axiovert 135; ZEISS, Oberkochen, Germany) and recorded by a digital camera (DXM 1200; Nikon, Tokyo, Japan).

Functional assessment of a prototype DDS. Cholesterol-containing di-palmitoylphosphatidylcholine (DPPC) liposomes including fluorescent dye were prepared as follows: Briefly, equimolar DPPC (Avanti, Alabaster, AL, USA) and cholesterol (Wako, Osaka, Japan) were dissolved in chloroform, then coated as a thin-layer on an eggplant flask by evaporation of the chloroform under reduced pressure. PBS containing 10 mM sodium fluorescein (uranine) was added to the eggplant flask and the PBS was sonicated at about 60˚C to form multilamellar vesicles (MLV). After five to six cycles of freeze–thawing of the MLV suspension, unilamellar vesicles (ULV; liposome) were prepared using a mini-extruder (Avanti) equipped with a 100 nm pore-size membrane filter (Whatman, Kent, England). Unincorporated fluorescent dye was removed by gel filtration on a Sephadex G50 column (GE Healthcare), and the liposome fractions were ultra-centrifuged (40,000 ×*g*) at 4˚C for 30 min in an Optima TL (Beckman, Brea, CA, USA), and the fluorescent liposomes recovered were re-suspended in PBS. Subsequently, in order to bind His-LTBP-CDC(ss)^{IP} to the fluorescent liposomes, they were incubated together in PBS at 25˚C for 30 min. After incubation, the fluorescent liposomes bound to His-LTBP-CDC(ss)^{IP} (designated as a prototype DDS) were harvested by ultra-centrifugation (40,000 ×*g*) at 4˚C for 30 min and were re-suspended in DMEM.

A549 cells were inoculated into a 24-well cell culture plate at 5×10^3 cells/well and cultured for 48 h. The prototype DDS was added to the cultured cells which were then incubated for 2 h, then washed with PBS. After interaction, the cells were fixed with 4% paraformaldehyde in PBS for 15 min at room temperature. Observation of the samples after PBS washing was conducted using a fluorescence microscope (Axiovert 135; ZEISS) and recorded by a digital camera (DXM 1200; Nikon).

Results

Expression and purification of recombinant chimera proteins. The purification of His-LTBP-CDC(ss)^{IP} and His-CDC(ss)^{IP} was conducted by standard nickel-affinity chromatography using Ni-NTA agarose (QIAGEN) or HisTrap HP (GE Healthcare). Both fractions containing purified His-LTBP-CDC(ss)^{IP} and His-CDC(ss)^{IP} were sufficiently pure as found by, CBB staining, on an SDS-PAGE gel [bands observed corresponding to 59.0 kDa for His-LTBP-CDC(ss)^{IP} and 56.7 kDa for His-CDC(ss)^{IP}; Figure 2A].

Binding ability of His-LTBP-CDC(ss)^{IP} to cholesterol-containing membranes. In order to confirm the binding ability of His-LTBP-CDC(ss)^{IP} to cholesterol-containing membranes, a binding assay to human erythrocyte cell membrane was conducted. His-LTBP-CDC(ss)^{IP} was detected only in the pellet fraction when in the presence of human erythrocyte membrane, in contrast to being detected in the supernatant when in the absence of human erythrocyte membrane (Figure 2B). These results demonstrate that His-LTBP-CDC(ss)^{IP}, a chimera protein composed of 1D-3D of ILY(ss) and 4D of Sm-hPAF, maintains high binding ability to cholesterol-containing membranes even after domain-swapping in 4D between ILY and Sm-hPAF and introduction of a structural addition at the *N*-terminal of 1D.

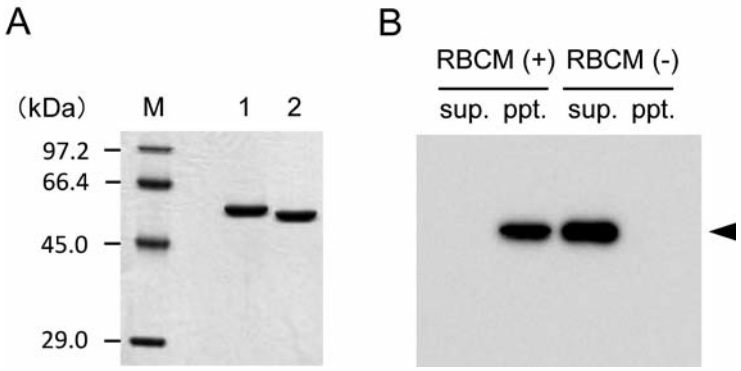

Figure 2. *Purification of the recombinant chimera proteins and the binding ability of His-LTBP-CDC(ss)^{IP} to cell membranes. A: Sodium dodecylsulphate-polyacrylamide gel electrophoresis (SDS-PAGE) image of the purified recombinant chimera proteins. M: Molecular weight marker, 1: His-LTBP-CDC(ss)^{IP}, 2: His-CDC(ss)^{IP}. B: Immunoblotting of His-LTBP-CDC(ss)^{IP} in the supernatant (sup.) and pellet (ppt.) fractions obtained by centrifugation of the reaction mixture containing His-LTBP-CDC(ss)^{IP}, with and without human erythrocyte membranes (RBCM). Arrowhead: His-LTBP-CDC(ss)^{IP}.*

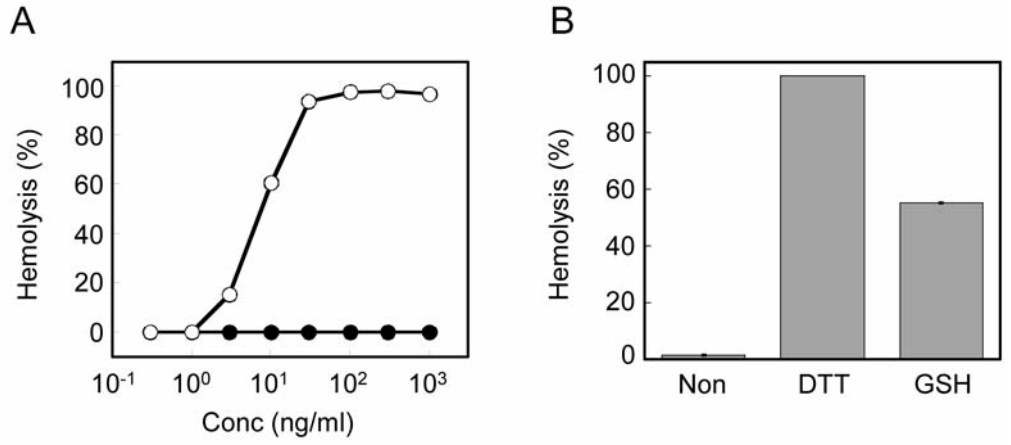

Figure 3. *Controlled pore-forming activity of His-LTBP-CDC(ss)^{IP}. A: Hemolytic activity of His-LTBP-CDC(ss)^{IP} on human erythrocytes under reducing (open symbol) and non-reducing conditions (closed symbol). These data indicate the average of two measurements. B: Hemolytic activity of His-LTBP-CDC(ss)^{IP} on human erythrocytes in the presence of artificial or physiological reductants [final concentration at 3 mM for dithiothreitol (DTT) and glutathione (reduced form) (GSH)]. Data indicate the average of two measurements.*

Controlled pore-forming activity of the recombinant chimera protein under reduced conditions. In order to investigate the controlled pore formation of His-LTBP-CDC(ss)^{IP}, the hemolytic activity of His-LTBP-CDC(ss)^{IP} was measured in the presence or absence of 10 mM DTT. His-LTBP-CDC(ss)^{IP} did not exhibit hemolytic activity even at a concentration of 1 μg/ml, under non-reduced conditions (Figure 3A). However, under reduced conditions with 10 mM DTT, His-LTBP-CDC(ss)^{IP} exhibited hemolysis at low concentrations, *i.e.* in the ng/ml range (Figure 3A), at a level of activity comparable to that of the parental molecule, ILY (8). These results demonstrate that His-LTBP-CDC(ss)^{IP} has controllable pore-forming activity that is expressed only in the reduced conditions.

The controlled pore-forming activity was further investigated using physiological reducing materials. The physiological reducing agent, the reduced form of glutathione (GSH), was added to the reaction mixture at the final concentration 3 mM to measure the hemolytic activity. In the presence of 3 mM GSH, His-LTBP-CDC(ss)^{IP} more than 50% hemolysis was observed (Figure 3B). This concentration of reduced GSH is similar to that found intracellularly *in vivo*. This result suggests that His-LTBP-CDC(ss)^{IP} would be able to express its controlled pore-forming activity inside target cells, and this property would enable His-LTBP-CDC(ss)^{IP} to form pores in the DDS carrier liposome membrane and deliver the drug, enclosed in the DDS carrier, exclusively into the target cells.

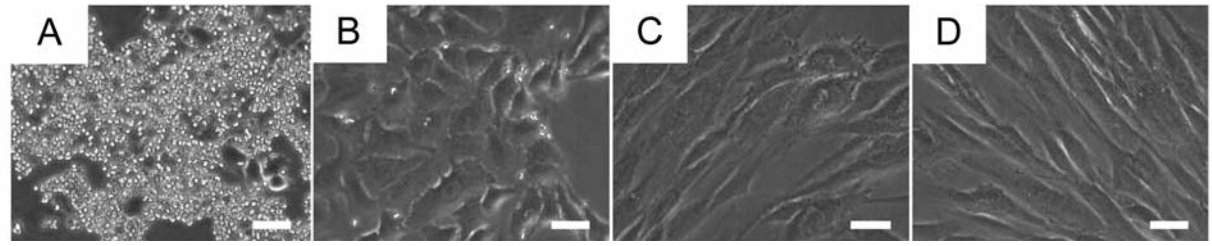

Figure 4. *Targeting of human lung tumor cells by the model drug-delivery system (DDS) tool. A: Human lung tumor cell line A549 incubated with the model DDS (His-LTBP-CDC(ss)^{IP} bound to human erythrocytes. The surface of A549 cells was covered with the erythrocytes delivered by His-LTBP-CDC(ss)^{IP}. B: A549 cells incubated with another model DDS consisting of a reference molecule without targeting domain [a targeting domain-lacking reference recombinant chimera protein, His-CDC(ss)^{IP} bound to human erythrocytes]. No erythrocytes were found on the surface of A549 cells. C: Human normal fibroblast cell line, NB1RGB incubated with the model DDS. D: NB1RGB cells incubated with another model DDS without targeting domain. Neither model DDS with nor without targeting domain were found on the surface of NB1RGB cells. Scale bars represent 40 μm.*

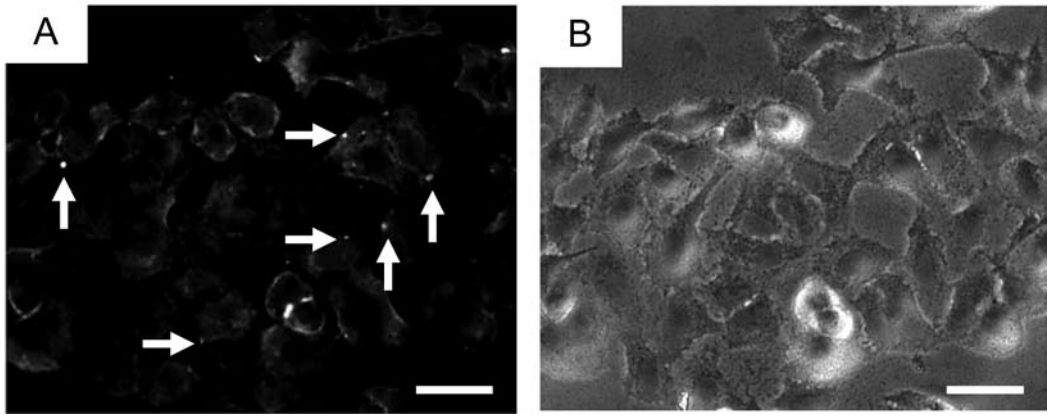

Figure 5. *Targeting of human lung tumor A549 cells by the prototype drug-delivery system (DDS) in vitro. Cholesterol-containing dipalmitoylphosphatidylcholine (DPPC) liposomes with enclosed fluorescent dye were bound with His-LTBP-CDC(ss)^{IP} to construct the prototype DDS. This prototype DDS was incubated with the human lung tumor cell line A549 and the bound/partially incorporated prototype DDS was observed by fluorescence microscopy. A: Fluorescent image of a typical field observed. Arrows indicate fluorescence spots due to the presence of prototype DDS. B: Bright-field image of A. Scale bars represent 40 μm.*

Evaluation for cell-specific targeting of a model DDS tool. A model DDS tool with a lung tumor-targeting domain, LTBP, was applied to human lung carcinoma A549 and human normal fibroblast NG1RGB in order to investigate target cell-specific delivery of His-LTBP-CDC(ss)^{IP} bound to fluorescence-labeled erythrocytes (designated as a model DDS). As shown by microscopy, the model DDS with the targeting domain LTBP successfully bound to human lung tumor A549 cells and delivered the erythrocytes (Figure 4A). Conversely, no erythrocytes were delivered to A549 cells by a reference molecule without the LTBP domain His-CDC(ss)^{IP} (Figure 4B). Moreover, no model DDS prepared using His-LTBP-CDC(ss)^{IP} or His-CDC(ss)^{IP} was delivered to human normal fibroblasts NB1RGB (Figures 4C and 4D). These results strongly suggest that His-LTBP-CDC(ss)^{IP} has the ability to deliver the cells/drug-carrier liposomes to target lung tumor cells *via* its targeting domain, LTBP.

Functional evaluation of prototype DDS. Finally, we investigated His-LTBP-CDC(ss)^{IP} as a potential vehicle for delivery of cholesterol-containing liposomes specifically to target cells. A prototype DDS was constructed using His-LTBP-CDC(ss)^{IP} together with a fluorescent dye (uranine) enclosed within cholesterol-containing liposomes. This construct enabled direct microscopic observation of the prototype DDS to the target cells. As shown in Figure 5, the liposomes which contained the fluorescent dye, were concentrated onto the human lung tumor A549 cells (indicated by arrows in Figure 5A). This suggests that the prototype DDS was successfully targeted and was able to bind to the target cells. Moreover, a significant part of the dye tended to disperse into the cytoplasm of target cells (Figure 5A). These observations suggest that this prototype DDS can be used for targeted delivery of the drug carrier and for the controlled release of the drug from the carrier into the

target cells under physiological reducing conditions, such as those occuring in the endolysosome.

Discussion

This study was conducted in order to develop a novel bacterial exotoxin-derived DDS tool as an effective approach for cancer and other clinical therapies. In this study, we chose a recombinant chimera protein based on a CDC member, ILY (8). To date, proposed applications of CDCs for clinical use have been reported only for the 4D of ILY, for an immunotherapy against cancer (15), an adjuvant for monoclonal antibody (mAb)-mediated complement-dependent cytolysis (16, 17), and for enhanced complement-mediated virolysis (18). To our knowledge, this is the first report utilizing an engineered CDC as a DDS into target cells. The recombinant chimera CDC, used in this study, was composed of 1D-3D of ILY(ss) with the introduction of an intramolecular disulfide bridge, together with 4D of Sm-hPAF, and displayed controlled pore formation, ensuring its safe use as a DDS tool. In order to apply this chimera CDC in this context, a lung tumor-binding peptide, designated as LTBP (14) was appended to the *N*-terminal of the protein and the resultant recombinant chimera protein was named His-LTBP-CDC(ss)^{IP} (Figure 1).

It has been reported that the pore formation by CDC is a result of structural changes in 1D-3D that are triggered by binding of 4D to the cell membrane (19). Although His-LTBP-CDC(ss)^{IP} was a chimera CDC composed of two different CDCs, namely 1D-3D of ILY(ss) and 4D of Sm-hPAF, the controlled pore formation activity, specifically under reduced conditions, was found to be at a level comparable to the unrestricted activity found in the parent molecule, ILY(ss) (data not shown). Indeed, the interchangeability of 4D between CDCs has been previously demonstrated by the substitution of 4D from ILY into SLO and pneumolysin (20). It is becoming apparent that the mode of receptor recognition in the CDC family varies: typical CDCs recognize membrane cholesterol as the receptor, while on the other hand, atypical CDCs, such as ILY, recognize human CD59 (huCD59) as their receptor (21). Moreover, the characteristics of 4D in many CDCs have also been revealed in previous studies (20, 22-23). From these and the data reported here, it is clear that substitution of CDC 4D can occur without loss of pore-forming activity, opening up the possibility for the selection of a particular 4D and design of the optimum chimera molecule depending on the desired DDS application. Furthermore, the *N*-terminus of the basic four-domain structures of CDC was clearly able to extend to allow another domain for protein/peptide or artificial molecules without pore-forming activity, as shown in the case of Sm-hPAF (GenBank ID: AB051299), the first five-domain type CDC whose extra *N*-terminal domain consists of ca. 160 amino acids. This observation suggested to us that it is possible to link a suitable targeting domain at the *N*-terminal of CDC to construct a DDS tool (Figure 1). As expected, the linkage of LTBP, a peptide showing high affinity for lung tumor cell lines (14), to the *N*-terminus of a CDC(ss)^{IP} had little or no detrimental effect on its binding to cell membranes (Figure 2B), nor on the controlled pore-forming activity (Figure 3) of the CDC(ss)^{IP}. Moreover, the ability of LTBP to specifically bind to human lung tumor cells was also maintained (Figure 4). Taken together, these results strongly suggest that protein engineering design of DDS tools with specific function is a promising strategy.

As shown in Figure 5, the fluorescence of a prototype DDS was observed both on and within the target cells and found to be concentrated (indicated by arrows in Figure 5A). This concentrated fluorescence suggests the enrichment of prototype DDS particles on the surface together with internalization to the cytoplasm of the target cells. Under physiological conditions such as those found within the endolysosome, His-LTBP-CDC(ss)^{IP} is able to undergo controlled self-disruption of the disulfide bridge between 2D and 3D (Figure 3B). These observations suggest that after internalization of the prototype DDS and the disruption of the His-LTBP-CDC(ss)^{IP} disulfide bridge, His-LTBP-CDC(ss)^{IP} can then exert its pore-forming activity, resulting in membrane pores on the cholesterol-containing liposomes (drug carrier) and in subsequent release of the liposomal contents, as indicated by the dispersed fluorescence, visible within the cells in Figure 5A. These results suggest His-LTBP-CDC(ss)^{IP} to be a promising molecule for use in lung cancer therapy.

In the present study, LTBP, with the ability to specifically bind to lung tumor cells, was selected as a targeting domain of a model DDS tool and for preparation of a prototype DDS. His-LTBP-CDC(ss)^{IP} was constructed as a model DDS tool and was shown to be promising for the purpose of lung tumor cell-specific targeting and for controlled intracellular drug release, leading to effective tumor cell death. If other targeting domains, such as an antibody or a single-chain variable fragment (scFv), specific for certain tumor antigen molecules were used in this model DDS tool, then the possibility arises of a diversity in tumor targets and a wide range of therapies against many other types of cancer.

Acknowledgements

This work was supported by KAKENHI [Grants-in-Aid for Scientific Research (C) 21590115] from the Ministry of Education, Culture, Sports, Science, and Technology of the Japanese Government, and by a Grant from the Institute of Technology and Science, The University of Tokushima Graduate School.

References

1 McClellan M, Benner J, Schilsky R, Epstein D, Woosley R, Friend S, Sidransky D, Geoghegan C and Kessler D: An accelerated pathway for targeted cancer therapies. Nat Rev Drug Discov *10*: 79-80, 2011.

2 Zhang W, Zhang Z and Zhang Y: The application of carbon nanotubes in target drug delivery systems for cancer therapies. Nanoscale Res Lett *6*: 555, 2011.

3 Wall DM, Srikanth CV and McCormick BA: Targeting tumors with *Salmonella typhimurium*–Potential for therapy. Oncotarget *1*: 721-728, 2010.

4 Oerlemans C, Bult W, Bos M, Storm G, Nijsen FW and Hennink WE: Polymeric micelles in anticancer therapy: targeting, imaging and triggered release. Pharm Res *27*: 2569-2589, 2010.

5 Lammers T, Hennink WE and Storm G: Tumour-targeted nanomedicines: principles and practice. Br J Cancer *99*: 392–397, 2008.

6 Patyar S, Joshi R, Prasad Byrav DS, Prakash A, Medhi B and Das BK: Bacteria in cancer therapy: a novel experimental strategy. J Biomed Sci *17*: 21, 2010.

7 Tweten RK: Cholesterol-dependent cytolysins, a family of versatile pore-forming toxins. Infect Immun *73*: 6199-6209, 2005.

8 Nagamune H, Ohnishi C, Katsuura A, Fushitani K, Whiley RA, Tsuji A and Matsuda Y: Intermedilysin, a novel cytotoxin specific for human cells secreted by *Streptococcus intermedius* UNS46 isolated from a human liver abscess. Infect Immun *64*: 3093-3100, 1996.

9 Ohkuni H, Todome Y, Okibayashi F, Watanabe Y, Ohtani N, Ishikawa T, Asano G and Kotani S: Purification and partial characterization of a novel human platelet aggregation factor in the extracellular products of *Streptococcus mitis*, strain Nm-65. FEMS Immunol Med Microbiol *17*: 121-129, 1997.

10 Hotze EM, Wilson-Kubalek EM, Rossjohn J, Parker MW, Johnson AE and Tweten RK: Arresting pore formation of a cholesterol-dependent cytolysin by disulfide trapping synchronizes the insertion of the transmembrane beta-sheet from a prepore intermediate. J Biol Chem *276*: 8261-8268, 2000.

11 Sekiya K, Akagi T, Tatsuta K, Sakakura E, Hashikawa T, Abe A and Nagamune H: Ultrastructural analysis of the membrame insertion of domain 3 of streptolysin O. Microbes Infect *9*: 1341-1350, 2007.

12 Ohkuni H, Nagamune H, Ozaki N, Tabata A, Todome Y, Watanabe Y, Takahashi H, Ohkura K, Kourai H, Ohtsuka H, Fischetii VA and Zabriskie JB: Characterization of recombinant *Streptococcus mitis*-derived human platelet aggregation factor. APMIS *120*: 56-71, 2012.

13 Farrand S, Hotze E, Friese P, Hollingshead SK, Smith DF, Cummings RD, Dale GL and Tweten RK: Characterization of a streptococcal cholesterol-dependent cytolysin with a lewis Y- and B-specific lectin domain. Biochemistry *47*: 7097-7107, 2008.

14 Oyama T, Sykes KF, Samli KN, Minna JD, Johnston SA and Brown KC: Isolation of lung tumor-specific peptides from a random peptide library: generation of diagnostic and cell-targeting reagents. Cancer Lett *202*: 219-230, 2003.

15 Nagamune H, Ohkura K, Umetsu K, Shouji H and Kourai H: A cell membrane modification technique using domain 4 of intermedilysin for immunotherapy against cancer. Anticancer Res *24*: 3367-3372, 2004.

16 Hu W, Ge X, You T, Xu T, Zhang J, Wu G, Peng Z, Chorev M, Aktas BH, Halperin JA, Brown JR and Qin X: Human CD59 inhibitor sensitizes rituximab-resistant lymphoma cells to complement-mediated cytolysis. Cancer Res *71*: 2298-2307, 2011.

17 You T, Hu W, Ge X, Shen J and Qin X: Application of a novel inhibitor of human CD59 for the enhancement of complement-dependent cytolysis on cancer cells. Cell Mol Immunol *8*: 157-163, 2011.

18 Hu W, Jin R, Zhang J, You T, Peng Z, Ge X, Bronson RT, Halperin JA, Loscalzo J and Qin X: The critical roles of platelet activation and reduced NO bioavailability in fatal pulmonary arterial hypertension in a murine hemolysis model. J Immunol *184*: 359-368, 2010.

19 Ramachandran R, Tweten RK and Johnson AE: Membrane-dependent conformational changes initiate cholesterol-dependent cytolysin oligomerization and intersubunit beta-strand alignment. Nat Struct Mol Biol *11*: 697-705, 2004.

20 Nagamune H, Ohkura K, Sukeno A, Cowan G, Mitchell TJ, Ito W, Ohnishi O, Hattori K, Yamato M, Hirota K, Miyake Y, Maeda T and Kourai H: The human-specific action of intermedilysin, a homolog of streptolysin O, is dictated by domain 4 of the protein. Microbiol Immunol *48*: 677-692, 2004.

21 Giddings KS, Zhao J, Sims PJ and Tweten RK: Human CD59 is a receptor for the cholesterol-dependent cytolysin intermedilysin. Nat Struct Mol Biol *11(12)*: 1173-1178, 2004.

22 Ohkura K, Hori H and Nagamune H: Molecular dynamics of human-specific cytolysin: analysis of membrane binding motif for therapeutic application. Anticancer Res *26*: 4055-4062, 2006.

23 Ohkura K, Nagamune H and Kourai H: Structural analysis of human specific cytolysin intermedilysin aiming application to cancer immunotherapy. Anticancer Res *24*: 3343-3353, 2004.

Received April 4, 2012
Revised May 13, 2012
Accepted May 14, 2012